ORIGINAL RESEARCH

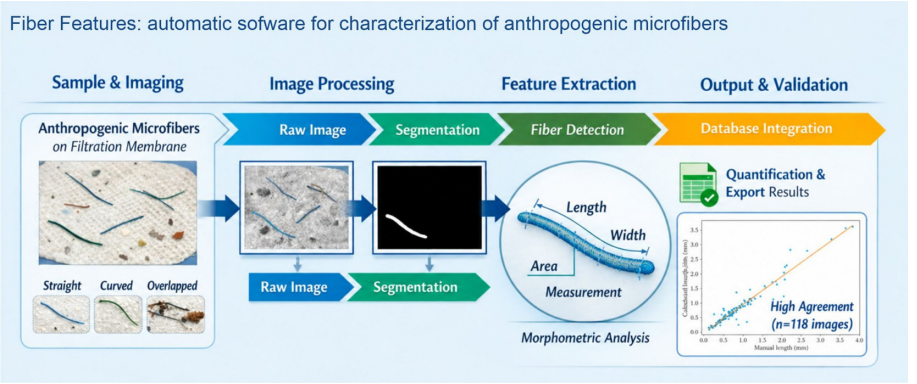
Fiber Features: a dedicated software for the automatic characterization of anthropogenic microfibers from environmental samples

Rosana P. Di Mauro[1, 2, *], Rodrigo E. Russo[3, *], Nadia M. Alves[1], Julieta S. Rodríguez[1], Julieta Rodriguez[1], Marina V. Diaz[1, 2, 4] and Juan I. Pastore[2, 3]

[1]Instituto Nacional de Investigación y Desarrollo Pesquero (INIDEP), Paseo Victoria Ocampo Nº 1, Escollera Norte, B7602HSA - Mar del Plata, Argentina. [2]Consejo Nacional de Investigaciones Científicas y Técnicas (CONICET), Argentina. [3]Laboratorio de Instrumentación Virtual y Robótica Aplicada (LIVRA-ICYTE), Departamento de Ingeniería Electrónica y Computación, Facultad de Ingeniería, Universidad Nacional de Mar del Plata (UNMdP), Juan B. Justo 4302, Mar del Plata, B7608FDQ, Argentina. [4]Instituto de Investigaciones Marinas y Costeras (IIMyC), Universidad Nacional de Mar del Plata (UNMdP), Consejo Nacional de Investigaciones Científicas y Técnicas (CONICET), Juan B. Justo 2550, B7608FBY - Mar del Plata, Argentina. ORCID *Rosana P. Di Mauro* https://orcid.org/0000-0002-8869-5534, *Rodrigo E. Russo* https://orcid.org/0009-0004-1798-0508, *Nadia M. Alves* https://orcid.org/0000-0002-8957-3133, *Julieta S. Rodríguez* https://orcid.org/0009-0002-0903-7267, *Julieta Rodriguez* https://orcid.org/0009-0009-8289-3810, *Marina V. Diaz* https://orcid.org/0000-0002-2912-5232, *Juan I. Pastore* https://orcid.org/0000-0002-5882-8957

Marine and Fishery Sciences MAFIS

GRAPHICAL ABSTRACT.



OPEN ACCESS

*Correspondence:
rosanam1877@gmail.com
rodrigo.e.russo@gmail.com

Received: 30 September 2026
Accepted: 23 October 2026

ISSN 2683-7595 (print)
ISSN 2683-7951 (online)

https://ojs.inidep.edu.ar

Journal of the Instituto Nacional de Investigación y Desarrollo Pesquero (INIDEP)

This work is licensed under a Creative Commons Attribution-NonCommercial-ShareAlike 4.0 International License

ABSTRACT. Microfibers (MFs) are among the most widespread forms of pollution in the environment. Standard procedures for counting and characterizing MFs typically involve particle extraction from the sampling matrix, filtration, and detailed inspection of the membranes to identify, classify, and characterize all detected items. Physical characterization often includes morphometric measurements such as surface area, length, and width, which significantly increases processing time. Recent advances in computer performance and digital imaging have greatly expanded the potential of image analysis as a tool for studying MFs from environmental samples. However, its broader adoption has been hindered by the challenges associated with automating the analysis process. In this study, we present a reliable and user-friendly software tool for the automatic detection, quantification, and measurement of MFs in digital images. The method was specifically developed for analyzing MFs retained on membranes used during filtration procedures, although its applicability may extend to other settings. The approach relies on the acquisition of high-resolution images, from which MFs are automatically segmented and measured in terms of length, width, and additional physical attributes. Results can be exported in multiple formats for further analysis. We evaluated the accuracy and repeatability of the

software by comparing its measurements with manual annotations across a dataset of 118 images. The results demonstrated a high level of agreement and robustness, highlighting the software's potential to streamline and standardize MF analysis in environmental research.

Key words: Marine pollution, automated image analysis, geodesic skeletal distance, morphometric characterization, weathering.

Fiber Features: un *software* especializado para la caracterización automática de microfibras antropogénicas a partir de muestras ambientales

RESUMEN. Las microfibras (MF) de origen antropogénico constituyen una de las formas de contaminación más extendidas en el medio ambiente. Los procedimientos estándar para el recuento y la caracterización de las MF suelen incluir la extracción de partículas de la matriz de muestreo, filtración y una inspección detallada de las membranas para identificar, clasificar y caracterizar todos los elementos detectados. La caracterización física a menudo comprende mediciones morfométricas, tales como el área superficial, la longitud y el ancho, lo cual incrementa considerablemente el tiempo de procesamiento. Los avances recientes en la capacidad de cómputo y la imagenología digital han ampliado notablemente el potencial del análisis de imágenes como herramienta para el estudio de las MF en muestras ambientales. No obstante, su adopción generalizada se ha visto limitada por los desafíos que conlleva la automatización del proceso de análisis. En este estudio, presentamos una herramienta de *software* robusta y fácil de usar para la detección, cuantificación y medición automáticas de MF en imágenes digitales. El método fue desarrollado específicamente para analizar MF retenidas en membranas utilizadas durante los procedimientos de filtración, si bien su aplicabilidad podría extenderse a otros contextos. El enfoque se basa en la obtención de imágenes de alta resolución, a partir de las cuales las MF se segmentan y miden automáticamente en función de su longitud, anchura y otros atributos físicos. Los resultados pueden exportarse en diversos formatos para su posterior análisis. Evaluamos la precisión y la repetibilidad del *software* comparando sus mediciones con anotaciones manuales en un conjunto de datos compuesto por 118 imágenes. Los resultados mostraron un alto grado de concordancia y robustez, lo que pone de relieve el potencial de este *software* para agilizar y estandarizar el análisis de MF en la investigación ambiental.

Palabras clave: Contaminación marina, análisis automatizado de imágenes, distancia esquelética geodésica, caracterización morfométrica, meteorización.

INTRODUCTION

Anthropogenic microfibers (MFs) are among the most prevalent forms of microplastic pollution in aquatic ecosystems (Barrows et al. 2018; Suaria et al. 2020; Lima et al. 2021), originating primarily from textile sources and wastewater discharges (Belzagui et al. 2020; Mishra et al. 2020), and occurring from coastal waters to the deep sea (Liu et al. 2022). Due to their small size and elongated morphology, MFs are readily ingested by zooplankton, bivalves, and fish, raising concerns about bioavailability, trophic transfer, and ecological impacts. Their morphometric properties, particularly length, width, and shape, strongly influence ingestion probability, retention time, and contaminant sorption capacity underscoring the importance of accurate and standardized dimensional measurements for ecological risk assessments (Koelmans et al. 2022).

Visual identification under microscopes remains one of the most used methods for MF quantification and characterization (Hidalgo-Ruz et al. 2012; Masura et al. 2015). Manual or semi-automated measurements, frequently performed using ImageJ or Fiji (Schindelin et al. 2012), enable the estimation of length, width, and surface area. However, these approaches are time-consuming, operator-dependent, and prone to variability, particularly when large numbers of particles must be processed. The lack of standardized, high-throughput procedures limits reproducibility and constrains comparative analyses across laboratories and monitoring programs.

Automated image analysis has been successfully applied to microplastic detection in beach

sediments and other matrices (Gauci et al. 2019; Lorenzo-Navarro et al. 2020). Nevertheless, many existing systems focus on particles larger than 1 mm or rely on costly instrumentation such as μFTIR imaging combined with machine learning (Primpke et al. 2017; Hufnagl et al. 2022). Several image-analysis tools have also been developed for the quantitative characterization of microplastics, including ImageJ/Fiji and shapeR, which provide image-processing and shape-descriptor analysis capabilities, and automated approaches such as TUM-ParticleTyper, designed for particle detection and morphological characterization (von der Esch et al. 2020; Valente et al. 2023). Although these tools offer valuable capabilities for particle analysis, their scope and implementation vary, and a comprehensive morphometric framework specifically tailored to elongated fibers remains necessary. In particular, accurate fiber characterization requires methods that account for curvature when estimating length and capture localized variations in width along the fiber. Although skeleton-based measurements can estimate fiber length along its curved trajectory, and object geometry can be used to derive width (Schnepf et al. 2023), these descriptors alone do not fully characterize longitudinal width heterogeneity. Therefore, a reproducible and scalable methodology that integrates these complementary measurements into a unified workflow remains needed (Liu et al. 2022).

To address these limitations, we developed Fiber Features (FF), a dedicated software tool for the automatic segmentation and morphometric characterization of MFs from digital images. The software integrates mathematical morphology and geodesic distance metrics constrained to the topological skeleton of each microfiber (Calabi and Hartnett 1968; Lantuéjoul and Maisonneuve 1984; Meyer 1989), enabling robust estimation of fiber length independently of curvature or orientation. In addition, FF provides width profiles along the skeletal path, allowing quantification of width variability and the objective assessment of surface weathering.

The objective of this study was to validate Fiber Features as a standardized and reproducible framework for automatic MF characterization and to evaluate its accuracy and repeatability relative to conventional manual image analysis methods. By providing a mathematically grounded and scalable approach, FF aims to support consistent morphometric datasets suitable for environmental monitoring and ecological research.

MATERIALS AND METHODS

Image library and manual characterization of anthropogenic microfibers

A subset of 118 digital images of MFs was randomly selected from an image library comprising 1,004 MF images, which were obtained from the gastrointestinal tracts of juvenile fish (Alves et al. 2024). This image library served both as the basis for the conceptual development of the software and for the subsequent evaluation of its performance.

Images were acquired using a 16-megapixel digital camera mounted on a stereomicroscope, capturing MFs retained on filtration membranes. During the filtration process, MFs can be deposited on the membrane surface plane in a range of positions and orientations; while some MFs remain relatively straight (Figure 1 A), others may be bent in the 2D plane (Figure 1 B) and overlapped with other MFs or particulate material (Figure 1 C), and out of focus sections due to bending in the 3D plane.

In addition, MFs may appear as relatively short strands (Figure 2 A), exhibit torsions (Figure 2 B), frayed edges or endings (Figure 2 C), and discoloration (Figure 2 D). These last descriptive features were annotated for the full characterization of the images in the reference library and used as qualitative indications of environmental weathering (Di Mauro et al. 2022, 2025).

Specifically, MFs simultaneously exhibiting discoloration (DSC) and frayed edges or endings (FYE) were classified as highly weathered (HW),

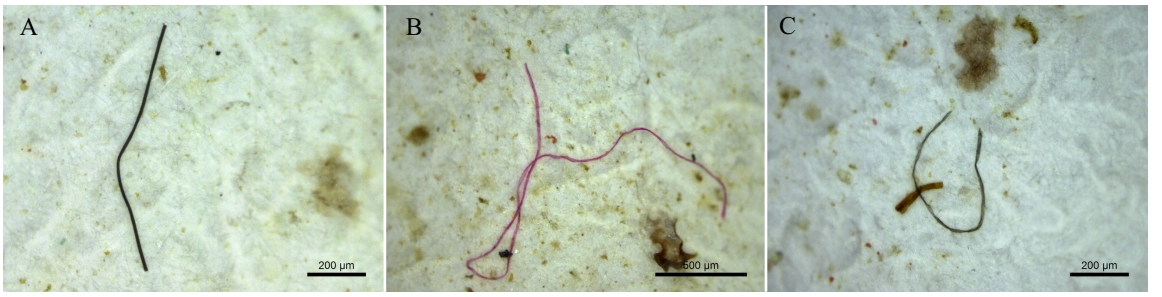


Figure 1. Example of the microfibers arrangement on the filtration membrane after the vacuum filtration process. Straight (A), bent (B), and overlapped with other particulate material (C).

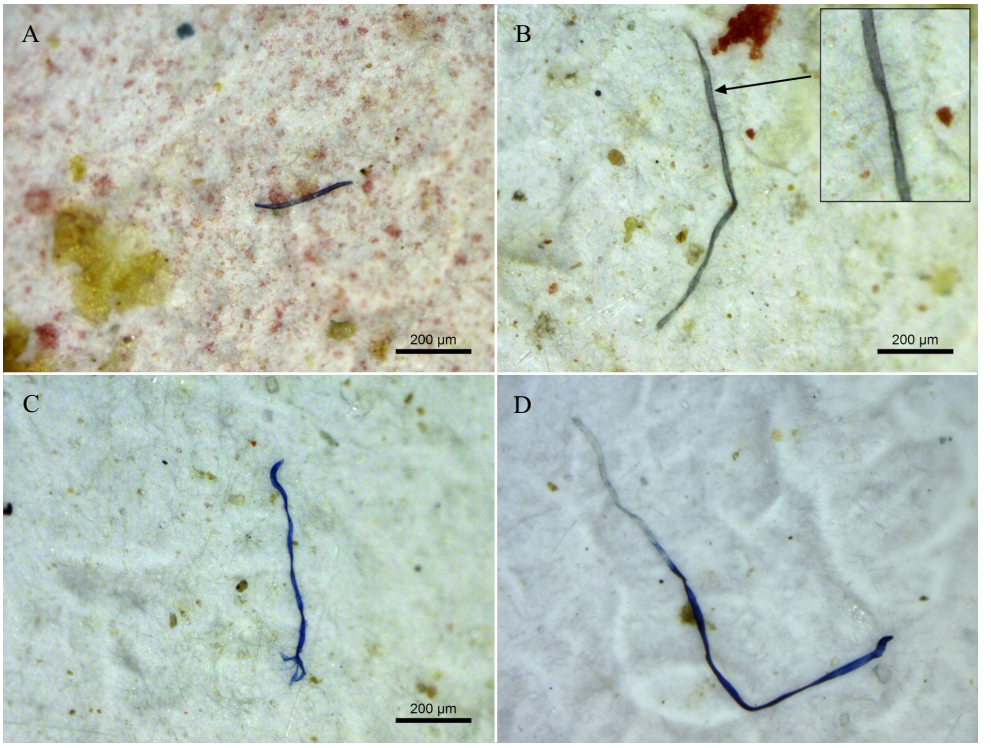


Figure 2. Examples of the anthropogenic microfibers showing morphological features annotated for the full characterization: short strands (A), surface with torsion (B), frayed edges or endings (C), and discoloration (D).

whereas those presenting only one of these features (either DSC or FYE) were classified as lightly weathered (LW). In addition, MFs lacking both features were considered minimally weathered (MW) (supplementary material, Table S1). This classification is consistent with the origin of the samples, as these were extracted from the gastrointestinal tracts of juvenile fish. Accordingly, MFs classified as MW were interpreted as having limited environmental exposure prior to ingestion, which is reflected in the absence of visible surface degradation features.

Manual measurements on each MF image were made using Fiji image analysis software (Schinde-

lin et al. 2012). Using the segmented polygon tool, a series of line segments was traced following the perimeter of each MF to generate a closed contour. From this contour, the surface area (SA, mm^2), perimeter (Pe) and Feret diameter (FD) were automatically measured, the latter being the distance (mm) between two tangents on opposite sides of the particle and parallel to a fixed dimension (Reinhardt 2021). For elongated and straight-positioned particles (Figure 1 A), FD can be considered a proxy for length, however, for MFs that are irregularly oriented on the 2D plane (Figure 1 B and 1 C), Pe and SA were used to estimate MF's length (LM) following the approach proposed by Elewa (2010):

$$L = \frac{\mathrm{Pe} + \sqrt{\mathrm{Pe}^2 - 16 \times \mathrm{SA}}}{4} \quad (1)$$

To ensure consistency in manually measured length (L_M), this formulation was applied uniformly to the entire dataset, regardless of MFs orientation.

Additionally, MF's width was manually measured (W_M) by drawing a straight line across a representative section of the fiber, which was selected based on clearly defined and well-resolved edges.

Automatic measurements with Fiber Features software

Fiber Features (FF) was designed to enable automatic image segmentation of digital images of MFs, and the subsequent measurement of various morphological parameters for their full characterization. The algorithms incorporate basic digital image processing techniques, mathematical morphology operators, and geodesic operators within a user-friendly interface. This purpose-specific software not only optimizes the automatic record of MF's shape and size, but it facilitates the documentation of other qualitative descriptors through a checkbox in the graphical user interface, with which users can specify MF's arrangement of the membrane surface, color and qualitative features of weathering, such as DSC and FYE, for a rapid and efficient documentation (supplementary material, Tutorial).

Among the automatic measurements provided by the software, the most relevant are length (L_{FF}) and width (W_{FF}), with the latter including the minimum, maximum, average values and the coefficient of variation (CV).

To consistently measure length in a reliable manner that can be applied to all MFs in a sample and represent MF's geometry, L_{FF} was defined as the geodesic distance measured between two endpoints constrained to the fiber's topological skeleton. The last is a simplified representation that preserves the basic structure of the original shape and remains equidistant from its borders. Furthermore, it emphasizes the geometric and topological properties of the shape, such as its connectivity, topology, direction, and width.

A formal definition of the skeleton suitable for both discrete and continuous domains was introduced by (Calabi and Hartnett 1968). It is based on the concept of maximal balls (Figure 3). A ball $B(x, r)$, centered at point x with radius r > 0, is defined as the set of all points within a given distance from x:

$$B(x, r) = \{y \in X: d(y, x) < r\} \quad (2)$$

A ball is maximal within shape O if it is not strictly contained in any other larger ball also entirely contained in O. The skeleton of O, denoted $Sk(O)$, consists of the centers of these maximal balls:

$$Sk(O) = \{x \in \mathrm{O}: B(x, r) \text{ is a maximal ball in } O\} \quad (3)$$

Sk results in a one-pixel wide structure that captures the essential shape of the object (Figure 4 B). To accurately determine the length of a fiber along its skeleton, FF was developed based on the concept of geodesic distance (Lantuéjoul and Maisonneuve 1984; Meyer 1989).

Let $O \subseteq \mathrm{X}$ be a shape within a binary image X.

The geodesic distance between two points p and q in O is defined as the length of the shortest path within O that connects them:

$$d_O(p, q) = \min_{\gamma \in \Gamma_O(p, q)} \{l(\gamma)\} \quad (4)$$

where $\Gamma_O(p, q)$ is the set of all paths in O joining p and q, and $l(\gamma)$ denotes the length of a path γ. If no such path exists, the distance is considered infinite.

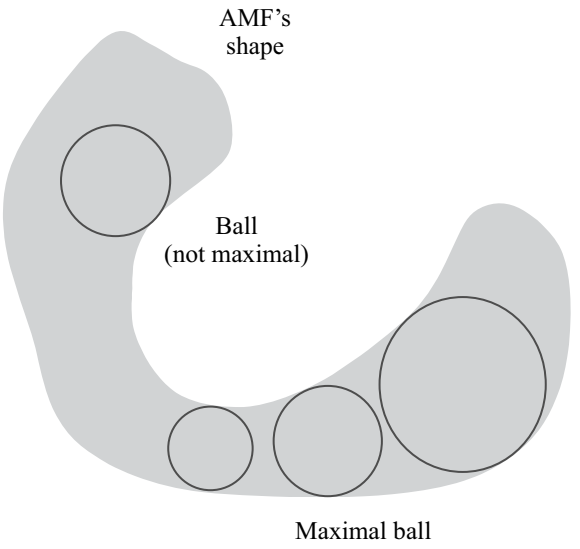


Figure 3. Conceptual diagram of maximal balls in an artificial anthropogenic microfiber.

Since we are particularly interested in paths that follow the medial axis of the structure, we define the skeletal geodesic distance as the geodesic distance restricted to the skeleton of O:

$$d_{\text{skel}}(p, q) = \min_{\gamma \in \Gamma_{\text{skel}}(p, q)} \{l(\gamma)\} \quad (5)$$

where $\Gamma_{\text{skel}}(p, q)$ denotes all paths in the skeleton that connect p and q. This definition of the skeletal geodesic distance provides the foundation for the quantitative assessment of MF's length with FF (L_{FF}) (Figure 4 C).

Once L_{FF} is established, W_{FF} can be derived based on the radii of the maximal balls positioned along the skeletal path. From the definition of the skeleton, each point on it corresponds to a unique maximal ball with a well-defined radius. Thus, the width profile of MFs can be derived from the set of diameters of the maximal balls along the geodesic arc:

$$A(O) = \{2r \mid B(x, r) \subseteq O \wedge B(x, r) \text{ is maximal in } O\} \quad (6)$$

This formulation enables a continuous and localized characterization of width along the entire structure, closely coupled with the definition of length via the geodesic arc on the skeleton (Equation 5).

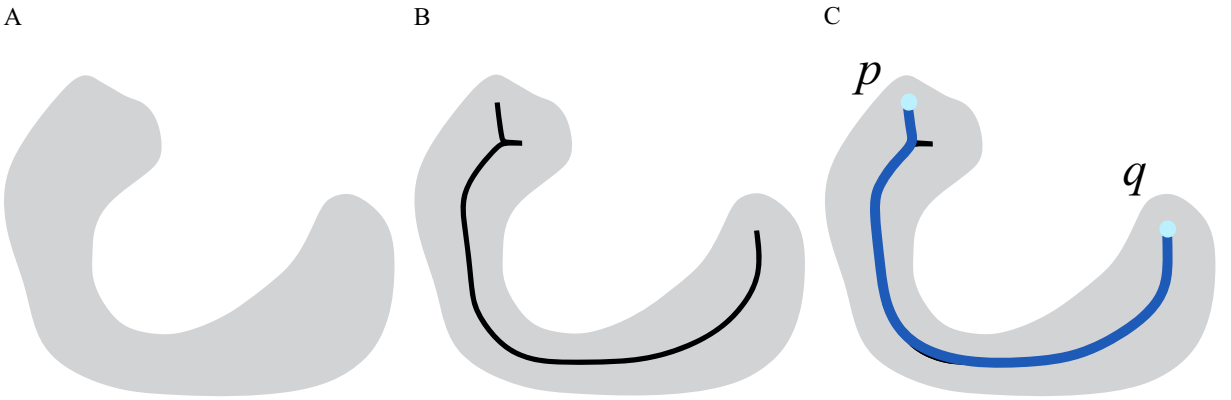


Figure 4. A) Artificial anthropogenic microfiber. B) Skeleton of an artificial anthropogenic microfiber. C) Geodesic skeletal distance between endpoints, measured along the skeleton.

Moreover, MFs presenting out of focus regions or contact artifacts (which prevent accurate W_{FF} measurement) are measured using area selection. This approach follows the same rationale as W_M measurement, in which a representative segment of the fiber is selected to capture its original cross-sectional shape. By focusing on well-resolved regions, the method ensures that W_{FF} estimates reflect the intrinsic fiber geometry while still allowing the assessment of width variability along the structure.

The radial aging index, a metric to quantify microfiber degrees of surface weathering

To quantitatively assess surface weathering, the Radial Aging Index (RAI) was defined as the CV of the widths measured point-by-point along the MF's morphological skeleton (Equation 3). Based on MF's qualitative classification into L_W and H_W, a CV threshold value was determined using an optimal cutoff approach to enable the objective automatic classification between the two classes. The threshold was estimated using a non-parametric approach based on empirical receiver operating characteristic (ROC) curves and the Youden index, a methodology widely applied in biomedical research to optimize classification performance (Schisterman et al. 2005). Greater diameter heterogeneity, with values above the threshold, was associated with higher surface weathering. To assess its robustness, its variability was further evaluated by resampling, using 100,000 simulations based on randomly sized subsets of the original data (supplementary material, Simulation).

Data analysis

Automatic measurements of length and width (L_{FF} and W_{FF}) were compared with manual measurements of the same parameters (L_M and W_M) by means of an ordinary least squares regression. To determine and visualize the threshold value of the RAI, the distributions of the CV of the widths were visualized using probability density plots. This allows direct comparison between unbalanced samples.

RESULTS AND DISCUSSION

Fiber Features (FF) successfully segmented and extracted morphometric features from most of the analyzed images (n = 118), demonstrating its capability to operate on typical MF images from environmental samples retained on filtration membranes. In a limited number of cases (n = 5), automated feature extraction was unsuccessful or yielded unreliable measurements due to specific image characteristics, including self-crossing fibers (Figure 1 B), overlapping structures (Figure 1 C), and out-of-focus regions (Figure 2 D). When a fiber crosses itself, the intersection creates shortcuts in the skeleton-based geodesic path, resulting in an underestimation of the actual fiber length. In addition, out-of-focus regions and overlapping structures can hinder the reliable identification of fiber boundaries, affecting width estimation and related morphometric parameters (supplementary material, Table S1). These cases highlight the limitations of automated morphometric analysis when image characteristics interfere with the reliable estimation of fiber length or width and should be considered when applying FF to complex environmental samples.

These conditions affected the stability of the skeleton reconstruction and, consequently, the calculation of geodesic length and width variability (supplementary material, Table S1). After excluding these cases, the comparison between L_{FF} and L_M measurements showed a high level of agreement, supporting the robustness of the geodesic skeletal approach for length estimation across fibers with variable curvature and orientation (Figure 5 A).

In contrast, differences observed between W_{FF} and W_M measurements (Figure 5 B) can be primarily attributable to the conceptual definition of each metric. W_M is inherently a localized measurement, obtained from a visually selected segment considered representative of the original fiber di-

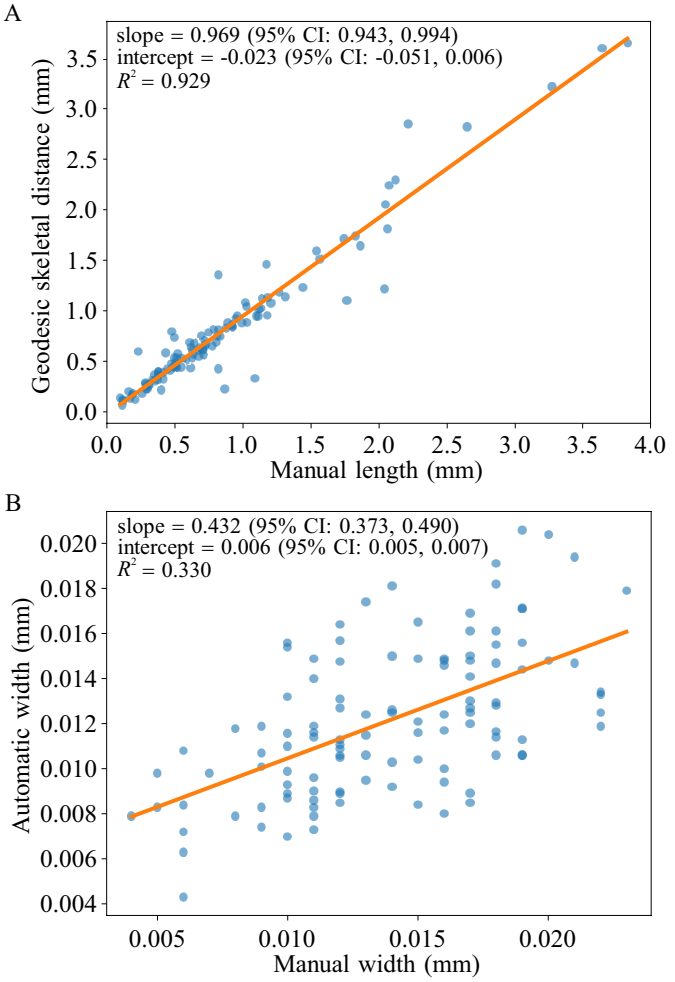


Figure 5. Validation of automated microfiber morphometric measurements obtained with FF against manual measurements. A) Comparison between manual microfiber Length and automated geodesic skeletal distance (mm). B) Comparison between manual Width and automatically estimated width (mm). Data points represent individual microfiber items.The orange line indicates the fitted linear regression. Reported statistics include slope, intercept, and coefficient of determination (R^2) with their corresponding 95% confidence intervals.

ameter. While this approach has been previously adopted, particularly to infer textile origin based on expected manufacturing diameters (Di Mauro et al. 2022; 2025), being approximately between 0.010 mm and 0.020 mm (Salvador Cesa et al. 2017; Dreillard et al. 2022; Xiao et al. 2023), it introduces subjectivity and does not capture longitudinal variability. Conversely, W_{FF} is a mean value derived from the distribution of diameters along the entire skeleton through the maximal ball formulation, providing a spatially integrated and objective characterization of width. As a result, W_{FF} not only estimates a representative mean diameter but also quantifies heterogeneity through the CV, which is inaccessible using conventional manual approaches.

A key methodological advancement of FF is the ability to characterize width variability as a continuous property along the fiber axis. However, this capability is sensitive to local segmentation arti-

facts. To address this limitation, an area-selection correction was implemented for MF items presenting localized distortions (e.g. out of focus sections, overlap, or bending). This correction follows the same rationale as W_M measurement, restricting analysis to well-resolved regions that preserve the original cross-sectional geometry of the MFs. As a result, the area-based approach acts as a targeted mechanism that removes artifact-driven distortions in diameter estimation while maintaining the capacity to assess variability (Figure 6).

The application of area correction improved the internal consistency of width measurements by reducing spurious fluctuations in the diameter profile. This effect is particularly relevant for the estimation of CV, which is highly sensitive to local extremes. By excluding unreliable segments, W_{FFcor} measurements yielded more interpretable estimates of radial heterogeneity, enhancing the overall quality of the dataset (Figure 6 C). Importantly, this approach allowed the inclusion of MFs that would otherwise be discarded, preserving statistical power while maintaining strict quality control.

The distribution of CV values derived from W_{FF} revealed a clear pattern associated with microfiber weathering (Figure 7 A). MFs classified as highly weathered (H_W) exhibited broader CV distributions, shifted toward higher values, indicating increased radial heterogeneity along the fiber axis. In contrast, lightly weathered (L_W) and minimally weathered (M_W) fibers displayed narrower distributions, reflecting more uniform diameter profiles. The comparison highlights the effect of area correction in reducing artifact-driven variability and improving the discrimination of radial heterogeneity across weathering states (Figure 7 B). This pattern is consistent with the expected effects of environmental degradation, including mechanical abrasion, fragmentation, and surface erosion, which introduce irregularities in fiber structure (Andrady 2011; Galloway et al. 2017; Liu et al. 2020). This is particularly relevant in the context of MFs pollution, where degradation dynamic is influenced by buoyancy and transport pathways, retention time and increasing the potential to absorb and transport chemical contaminants or microorganisms (Liu et al. 2020; Peng et al. 2026). Standardizing weathering as 'aging' assessment has implications for ecotoxicological evaluations and for understanding spatiotemporal patterns of MFs persistence across ecosystems. Furthermore, MFs are widely recognized as the dominant type of anthropogenic pollution in aquatic environments (Liu et al. 2022; Li et al. 2023). Their widespread presence, persistence, and capacity to be ingested across multiple trophic levels highlight the need for standardized and scalable analytical tools to assess bioavailability (Duncan et al. 2017).

The definition of the Radial Aging Index (RAI) as the mean CV along the fiber skeleton provides a quantitative descriptor of this process. The ROC-based analysis identified a threshold value (RAI = 0.34) that effectively discriminates between L_W and H_W MFs, with stable performance under resampling (Figure 8). For future datasets, this threshold value has to be estimated and revalidated. This result demonstrates that width variability, as captured through the skeletal framework, contains sufficient information to objectively classify MF's weathering states. The inclusion of MW fibers derived from gastrointestinal samples of juvenile fish provides an ecologically meaningful baseline, representing MF items with limited environmental exposure prior to ingestion. Their consistently low CV values reinforce the interpretation of RAI as a proxy for progressive environmental alteration.

From a methodological perspective, the integration of geodesic skeletal analysis with maximal ball-based width estimation represents a significant advancement over existing manual or semi-automated approaches associated with operator-dependent biases (Russ and Dehoff 2000; Cowger et al. 2020). Unlike traditional metrics that rely on simplified geometric proxies (e.g. Feret diameter), the FF framework preserves the intrinsic topology of the fibers and enables measurement invariance with respect to curvature and

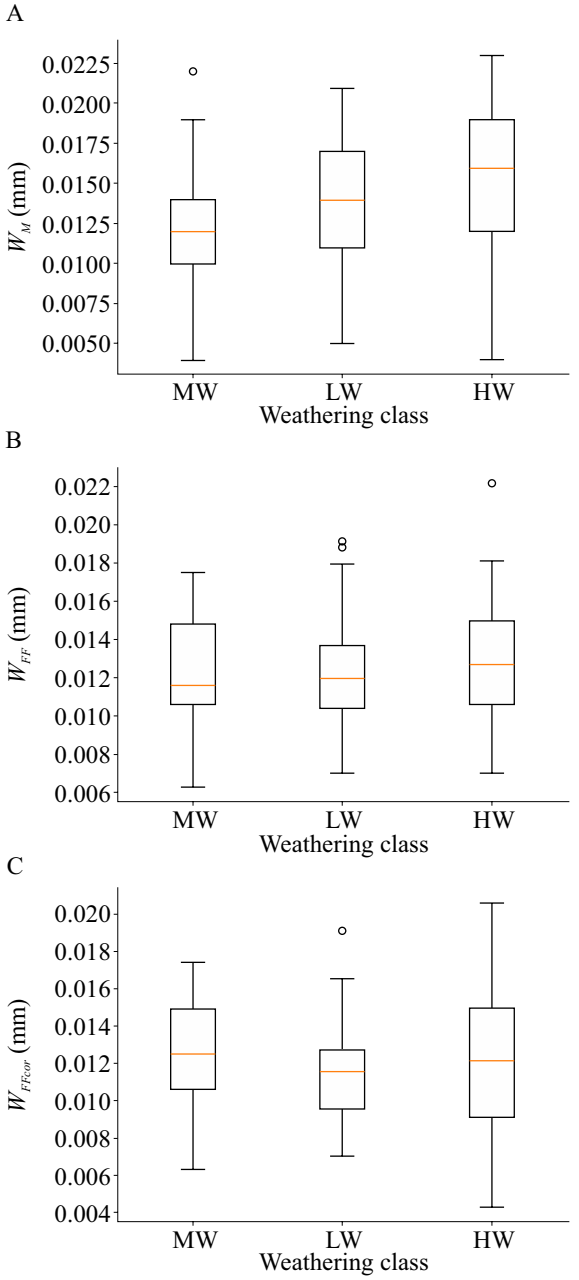


Figure 6. Boxplot showing width distributions for each group of microfibers classified into minimally weathered (MW), lightly weathered (LW) and highly weathered (HW). A) Distributions of manual width (W_M). B) Distribution of mean width estimated by Fiber Features (W_{FF}). C) Distribution of corrected mean width estimated by Fiber Features software with area selection (W_{FFcor}).

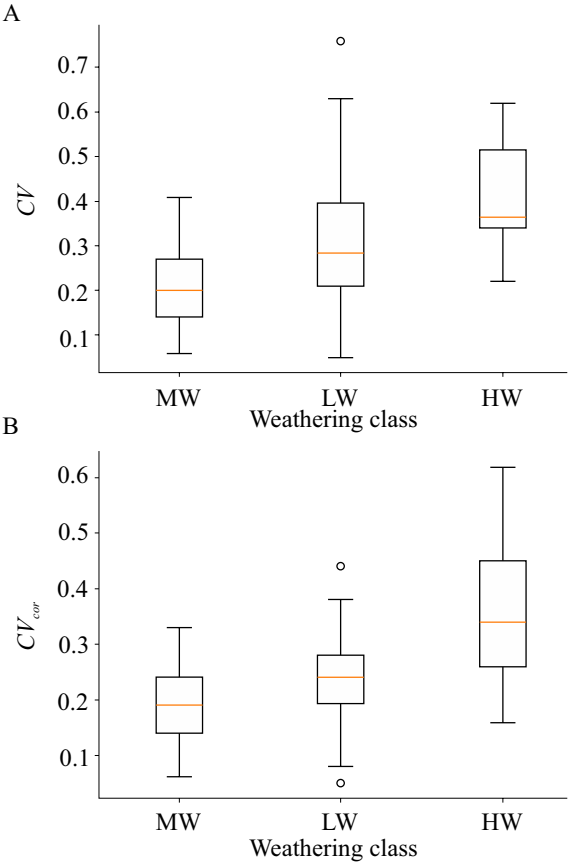


Figure 7. Distribution of the coefficient of variation (CV) of microfiber width as a function of weathering state. CV values derived from automated width measurements (W_{FF}) (A), and CV values derived from corrected width measurements (W_{FFcor}) after applying area-selection (B). Weathering classes include minimally weathered (MW), lightly weathered (LW), and highly weathered (HW) microfibers.

orientation. This is particularly relevant for environmental samples, where MFs rarely conform to idealized straight geometries (Masura et al. 2015; Suaria et al. 2020).

Furthermore, the standardization of measurements using FF reduces operator-dependent variability and enhances reproducibility across datasets. This is critical for scaling MFs research toward large monitoring programs, where comparability between studies is often limited by methodological inconsistencies. By generating harmonized mor-

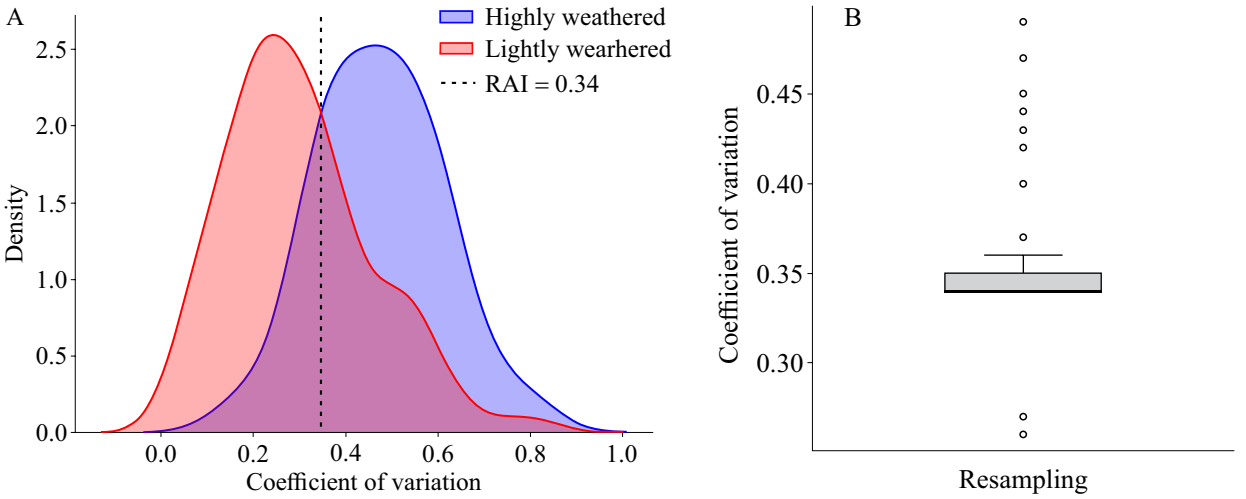


Figure 8. Distribution of the coefficient of variation (CV) of the microfiber width (W_{FFcor}) used as an index of radial aging. A) Density plots show the distribution of CV values calculated along the microfiber longitudinal axis for lightly weathered (L_W) in red and highly weathered (H_W) microfibers in blue. The dashed vertical line indicates the threshold value of the Radial Aging Index (RAI = 0.34) to quantitatively separate both classes. B) Boxplot related to the threshold value variability (median = 0.34, interquartile range: 0.34-0.35, range: 0.26-0.50).

phometric datasets, FF facilitates downstream applications such as statistical modeling, meta-analysis, and probabilistic risk assessment (Kooi and Koelmans 2019; Koelmans et al. 2020).

Despite its strengths, the performance of FF remains dependent on image quality and segmentation reliability. Complex environmental matrices, such as filters with high organic content or particle overlaps, may introduce noise that affects skeleton extraction and width estimation. Future developments should focus on improving segmentation robustness under such imaging conditions, potentially through adaptive thresholding or machine learning-based preprocessing.

Overall, the results demonstrate that FF provides a robust, scalable, and conceptually consistent framework for MFs morphometric characterization. By combining automated image analysis with mathematically grounded descriptors of shape and variability, the method enables a more comprehensive understanding of MFs morphological structure and their transformation under environmental exposure. This represents a critical step toward the standardization of MFs measurements and the integration of morphometric data into ecological and risk assessment frameworks.

Funding

This study was supported by the Instituto Nacional de Investigación y Desarrollo Pesquero (INIDEP), Consejo Nacional de Investigaciones Científicas y Técnicas (CONICET-PIP11220200102831CO) and Fondo para la Investigación Científica y Tecnológica (FONCYT-PICT 2020-03022). This is INIDEP contribution no 2556.

Data availability statement

Data can be made available upon request.

Declaration of competing interest

The authors declare that they have no known competing financial interests or personal relationships that could have appeared to influence the work reported in this paper.

Declaration on the use of AI and automated tools

During the preparation of this work the authors used ChatGPT (OpenAI, GPT-5) to assist in language editing and improvement of grammar and fluency. After using this tool, the authors reviewed and edited the content as needed and took full responsibility for the content of the publication.

Author contributions

Rosana P. Di Mauro: conceptualization; data curation; formal analysis; investigation; methodology; writing-original draft. Rodrigo E. Russo: methodology; software; visualization; validation; writing-review and editing. Nadia M. Alves: methodology; data curation; formal analysis; investigation; writing-original draft; writing-review and editing. Julieta S. Rodríguez: methodology; writing-original draft; writing-review and editing. Julieta Rodriguez: methodology. Marina V. Diaz: funding acquisition; writing-original draft; writing-review and editing. Juan I. Pastore: conceptualization; investigation; methodology; software; visualization; validation; formal analysis; writing-original draft; writing-review and editing.

REFERENCES

Alves NM, Rodriguez J, Di Mauro R, Rodríguez JS, Maldonado D, Braverman MS, Temperoni B, Diaz MV. 2024. Like noodles in a soup: anthropogenic microfibers are being ingested by juvenile fish in nursery grounds of the southwestern Atlantic ocean. Mar Pollut Bull. 202: 116368. DOI: https://doi.org/10.1016/j.marpolbul.2024.116368

Andrady AL. 2011. Microplastics in the marine environment. Mar Pollut Bull. 62 (8): 1596-1605. DOI: https://doi.org/10.1016/j.marpolbul.2011.05.030

Barrows APW, Cathey SE, Petersen CW. 2018. Marine environment microfiber contamination: global patterns and the diversity of microparticle origins. Environ Pollut. 237: 275-284. DOI: https://doi.org/10.1016/j.envpol.2018.02.062

Belzagui F, Gutiérrez-Bouzán C, Álvarez-Sánchez A, Vilaseca M. 2020. Textile microfibers reaching aquatic environments: a new estimation approach. Environ Pollut. 265: 114889. DOI: https://doi.org/10.1016/j.envpol.2020.114889

Calabi L, Hartnett WE. 1968. Shape recognition, prairie fires, convex deficiencies and skeletons. Am Math Mon. 75: 335-342.

Cowger W, Booth A, Hamilton B, Primpke S, Munno K, Lusher A, Dehaut A, Vaz VP, Liboiron M, Devriese LI, et al. 2020. Reporting guidelines to increase the reproducibility and comparability of research on microplastics. Appl Spectrosc. 74 (9): 1066-1077. DOI: https://doi.org/10.1177/0003702820930292

Di Mauro R, Alves N, Rodriguez J, Sobrero L, Chiesa I, Hozbor M, Allega L, Antacli J, Diaz MV, Schiariti A. 2025. Assessing anthropogenic microfiber pollution in the southwestern Atlantic Ocean: a large-scale study on spatial distribution, concentration, and physical characterization. Environ Sci Pollut Res. 32: 22458-22478. DOI: https://doi.org/10.1007/s11356-025-36964-6

Di Mauro R, Castillo S, Perez A, Iachetti C, Silva L, Tomba JP, Chiesa I. 2022. Anthropogenic microfibers are highly abundant at the Burdwood Bank seamount, a protected Sub-Antarctic environment in the Southwestern Atlantic Ocean. Environ Pollut. 306. DOI: https://doi.org/10.1016/j.envpol.2022.119364

Dreillard M, Barros C De F, Rouchon V, Emonnot C, Lefebvre V, Moreaud M, Guillaume D, Rimbault F, Pagerey F. 2022. Quantification and morphological characterization of microfibers emitted from textile washing. Sci Total Environ. 832: 154973. DOI: https://doi.org/10.1016/j.scitotenv.2022.154973

Duncan E, Botterell Z, Broderick A, Galloway T, Lindeque P, Nuno A, Godley B. 2017. A global review of marine turtle entanglement in anthropogenic debris: a baseline for further action. Endanger Species Res. 34: 431-448. DOI: https://doi.org/10.3354/esr00865

Elewa A. 2010. Morphometrics for nonmorphometricians. DOI: https://doi.org/10.1007/978-3-540-95853-6

Galloway T, Cole M, Lewis C. 2017. Interactions of microplastic debris throughout the marine ecosystem. Nat Ecol Evol. 1: 0116. DOI: https://doi.org/10.1038/s41559-017-0116

Gauci A, Deidun A, Montebello J, Abela J, Galgani F. 2019. Automating the characterisation of beach microplastics through the application of image analyses. Ocean Coast Manage. 182: 104950. DOI: https://doi.org/10.1016/j.ocecoaman.2019.104950

Hidalgo-Ruz V, Gutow L, Thompson RC, Thiel M. 2012. Microplastics in the marine environment: a review of the methods used for identification and quantification. Environ Sci Technol. 46 (6): 3060-3075. DOI: https://doi.org/10.1021/es2031505

Hufnagl B, Stibi M, Martirosyan H, Wilczek U, Möller JN, Löder MGJ, Laforsch C, Lohninger H. 2022. Computer-assisted analysis of microplastics in environmental samples based on μftir imaging in combination with machine learning. Environ Sci Technol Lett. 9 (1): 90-95. DOI: https://doi.org/10.1021/acs.estlett.1c00851

Koelmans A, Redondo-Hasselerharm P, Hazimah N, Kooi M. 2020. Solving the non-alignment of methods and approaches used in microplastic research in order to consistently characterize risk. Environ Sci Technol. 54 (19): 12307-12315. DOI: https://doi.org/10.1021/acs.est.0c02982

Koelmans AA, Redondo-Hasselerharm PE, Nor NHM, de Ruijter VN, Mintenig SM, Kooi M. 2022. Risk assessment of microplastic particles. Nat Rev Mater. 7 (2): 138-152.

Kooi M, Koelmans AA. 2019. Simplifying microplastic via continuous probability distributions for size, shape, and density. Environ Sci Technol Lett. 6 (9): 551-557. DOI: https://doi.org/10.1021/acs.estlett.9b00379

Lantuéjoul C, Maisonneuve F. 1984. Geodesic methods in image analysis. Pattern Recognit. 17 (2): 177-187.

Li Y, Lu Q, Xing Y, Liu K, Ling W, Yang J, Yang Q, Wu T, Zhang J, Pei Z, Gao Z, Li X, Yang F, Ma H, Liu K, Zhao D. Review of research on migration, distribution, biological effects, and analytical methods of microfibers in the environment. Sci Total Environ. 855: 158922. DOI: https://doi.org/10.1016/j.scitotenv.2022.158922

Lima ARA, Ferreira GVB, Barrows APW, Christiansen KS, Treinish G, Toshack MC. 2021. Global patterns for the spatial distribution of floating microfibers: Arctic Ocean as a potential accumulation zone. J Hazard Mat. 403: 123796. DOI: https://doi.org/10.1016/j.jhazmat.2020.123796

Liu J, Qiang L, An L, Wang M, Qingbo Y, Zhu B, Ding J, Ye C, Xu Y. 2022. Microfiber pollution in the earth system. Rev Environ Contam Toxicol. 260. DOI: https://doi.org/10.1007/s44169-022-00015-9

Liu P, Zhan X, Wu X, Li J, Wang H, Gao S. 2020. Effect of weathering on environmental behavior of microplastics: properties, sorption and potential risks. Chemosphere. 242: 125193. DOI: https://doi.org/10.1016/j.chemosphere.2019.125193

Lorenzo-Navarro J, Castrillón-Santana M, Santesarti E, De Marsico M, Martínez I, Raymond E, Gómez M, Herrera A. 2020. Smacc: a system for microplastics automatic counting and classification. IEEE Access. 8: 25249-25261. DOI: https://doi.org/10.1109/ACCESS.2020.2970498

Masura J, Baker JE, Foster GD, Arthur C, Herring C. 2015. Laboratory methods for the analysis of microplastics in the marine environment: recommendations for quantifying syn-

thetic particles in waters and sediments. NOAA Tech Mem NOS-OR&R. 48. https://repository.library.noaa.gov/view/noaa/10296/noaa_10296_DS1.pdf.

Meyer F. 1989. Skeletons and perceptual graphs. Signal Process. 16 (4): 335-363. DOI: https://doi.org/10.1016/0165-1684(89)90030-3

Mishra S, Singh RP, Rath CC, Das AP. 2020. Synthetic microfibers: source, transport and their remediation. J Water Process Eng. 38: 101612. DOI: https://doi.org/10.1016/j.jwpe.2020.101612

Peng L, Zheng N, Li Y, An Q, Chen C, Xiu Z, Li X, Wei Y. 2026. Dynamic evolution of microbial colonization on indoor microplastics: Polymer diversity-driven co-occurrence networks and health risks. Environ Int. 207: 109994. DOI: https://doi.org/10.1016/j.envint.2025.109994.

Primpke S, Lorenz C, Rascher-Friesenhausen R, Gerdts G. 2017. An automated approach for microplastics analysis using focal plane array (fpa) ftir microscopy and image analysis. Anal Methods. 9 (9): 1499-1511.

Reinhardt I. 2021. Modellierung der partikelcharakteristika von mikroplastik im boden: modelling of features of microplastics in soil [dissertation]. Universität Stuttgart.

Russ JC, Dehoff RT. 2000. Basic stereological procedures. Springer US.

Salvador Cesa F, Turra A, Baruque-Ramos J. 2017. Synthetic fibers as microplastics in the marine environment: a review from textile perspective with a focus on domestic washings. Sci Total Environ. 598: 1116-1129. DOI: https://doi.org/10.1016/j.scitotenv.2017.04.172

Schindelin J, Arganda-Carreras I, Frise E, Kaynig V, Longair M, Pietzsch T, Preibisch S, Rueden C, Saalfeld S, Schmid B, et al. 2012. Fiji: an open-source platform for biological image analysis. Nat Methods. 9: 676-82. DOI: https://doi.org/10.1038/nmeth.2019

Schisterman E, Perkins N, Liu A, Bondell H. 2005. Optimal cut-point and its corresponding youden index to discriminate individuals using pooled blood samples. Epidemiology. 16: 73-81. DOI: https://doi.org/10.1097/01.ede.0000147512.81966.ba

Schnepf U, Lioba von Moers-Messmer MA, Brümmer F. 2023. A practical primer for image-based particle measurements in microplastic research. Microplast Nanoplast. 3: 16. DOI: https://doi.org/10.1186/s43591-023-00064-4

Suaria G, Achtypi A, Perold V, Lee JR, Pierucci A, Bornman TG, Aliani S, Ryan PG. 2020. Microfibers in oceanic surface waters: a global characterization. Sci Adv. 6 (23): eaay8493. DOI: https://doi.org/10.1126/sciadv.aay8493

Valente T, Ventura D, Matiddi M, Sbrana A, Silvestri C, Piermarini R, Jacomini C, Costantini ML. 2023. Image processing tools in the study of environmental contamination by microplastics: reliability and perspectives. Environ Sci Pollut Res. 30: 298-309. DOI: https://doi.org/10.1007/s11356-022-22128-3

von der Esch E, Kohles AJ, Anger PM, Hoppe R, Niessner R, Elsner M, Ivleva NP. 2020. TUM-ParticleTyper: a detection and quantification tool for automated analysis of (microplastic) particles and fibers. PLoS ONE. 15 (6): e0234766. DOI: https://doi.org/10.1371/journal.pone.0234766

Xiao S, Cui Y, Brahney J, Mahowald NM, Li Q. 2023. Long-distance atmospheric transport of microplastic fibres influenced by their shapes. Nat Geosci. 16 (10): 863-870.